

Equation of State for Neutron Stars in the Quark-Meson Coupling Model with the Cloudy Bag

Tsuyoshi MIYATSU and Koichi SAITO

*Department of Physics, Faculty of Science and Technology, Tokyo University of Science, Noda
278-8510, Japan*

E-mail: tsuyoshi.miyatsu@rs.tus.ac.jp

(Received January 25, 2019)

Using the quark-meson coupling model with the cloudy bag, we construct the equation of state for neutron stars with hyperons in SU(3) flavor symmetry. The hyperfine interaction due to the gluon exchange and the pion-cloud effect inside a baryon is taken into account in vacuum and nuclear matter. We investigate how the quark degrees of freedom and the exchanges of gluon and pion between two quarks affect the properties of nuclear and neutron-star matter. It is found that the variation of baryon substructure in matter plays an important role in supporting massive neutron stars.

KEYWORDS: equation of state, dense nuclear matter, neutron stars, hyperons

1. Introduction

Many theoretical discussions on the properties of nuclear matter have been studied so far, where protons and neutrons are generally treated as point-like objects as in Quantum Hadrodynamics (QHD) [1]. However, it is apparent that baryons are composed of quarks and gluons. There are a few calculations in which the quark degrees of freedom inside a baryon and the variation of baryon substructure in matter are considered.

Thanks to the recent advances in astrophysical observations, we can get some precise information on the properties of neutron stars. In particular, the discovery of massive neutron stars [2, 3] is very useful to construct the equation of state (EoS) for dense nuclear matter. In addition, the gravitational wave from binary neutron star detected by LIGO and Virgo scientific collaborations [4] is also important to make a constraint on the EoS for neutron stars.

In the present study, we consider the baryon substructure due to quarks using the quark-meson coupling (QMC) model [5–7], and construct the EoS for neutron stars with hyperons, which can satisfy with both nuclear properties and astrophysical observations.

2. Matter Description at the Quark-Mean Field Level

Using the volume coupling version of the cloudy bag model (CBM) [8], the hyperfine interaction due to the gluon exchange and the pion-cloud effect inside a baryon can be taken into account. The mass for baryon (B) with the one-gluon and one-pion exchange effects (ΔE_g and ΔE_π) is described by $M_B = E_{\text{MIT}} + \Delta E_g + \Delta E_\pi$, where E_{MIT} is the bag energy based on the MIT bag model. The calculation of baryon spectra is well tuned so as to fit the mass differences between N , Δ , and Ω in vacuum [9, 10].

In order to describe nuclear matter, we need the intermediate attractive and short-range repulsive nuclear forces. As in the case of QHD, it is achieved by introducing the σ and ω mesons. In addition, the strange mesons (σ^* and ϕ) and ρ meson are included. The effect of the baryon substructure is then

Table I. Values of a_B , b_B , a'_B and b'_B in the QMC, QMCg and CQMC models.

B	(a) QMC				(b) QMCg				(c) CQMC			
	a_B (fm)	b_B	a'_B (fm)	b'_B	a_B (fm)	b_B	a'_B (fm)	b'_B	a_B (fm)	b_B	a'_B (fm)	b'_B
N	0.179	1.00	—	—	0.167	1.12	—	—	0.118	1.04	—	—
Λ	0.172	1.00	0.220	1.00	0.160	1.17	0.270	1.00	0.122	1.09	0.290	1.00
Σ	0.177	1.00	0.223	1.00	0.188	1.04	0.240	1.18	0.184	1.02	0.277	1.15
Ξ	0.166	1.00	0.215	1.00	0.176	1.19	0.267	1.05	0.181	1.15	0.292	1.04
Δ	0.196	1.00	—	—	0.216	0.89	—	—	0.197	0.89	—	—

taken into account through two kind of scalar polarizabilities:

$$C_B(\sigma) = -\frac{1}{g_{\sigma B}} \left(\frac{\partial M_B^*}{\partial \sigma} \right), \quad C'_B(\sigma^*) = -\frac{1}{g_{\sigma^* B}} \left(\frac{\partial M_B^*}{\partial \sigma^*} \right), \quad (1)$$

where the effective baryon mass, M_B^* , is calculated by the CBM model, and $g_{\sigma B}$ and $g_{\sigma^* B}$ are the σ - B and σ^* - B coupling constants, respectively.

3. Field-Dependent Coupling Constants in the QMC Model

In the QMC model, it has been known that the scalar polarizabilities decrease linearly as the total baryon density, ρ_B , increases [11]. In the present study, we employ the following, field-dependent, simple parametrizations for them [12]:

$$C_B(\sigma) = b_B [1 - a_B (g_{\sigma N} \sigma)], \quad C'_B(\sigma^*) = b'_B [1 - a'_B (g_{\sigma^* \Lambda} \sigma^*)], \quad (2)$$

where $g_{\sigma N}$ and $g_{\sigma^* \Lambda}$ are respectively the σ - N and σ^* - Λ coupling constants at zero density, and the parameters a_B , b_B , a'_B , and b'_B are tabulated in Table I. We here present three cases: (a) the QMC model without gluons and pions, (b) the QMC model with the gluon interaction, denoted by QMCg, and (c) the QMC model with the gluon and pion interactions based on the chiral quark-meson coupling (CQMC) model [9]. The effect of the variation of baryon structure at the quark level can be described with the parameters a_B and a'_B . In addition, the extra parameters, b_B and b'_B , are necessary to express the effect of hyperfine interaction between two quarks. Using these linear form, we can obtain the field-dependent coupling constants for the scalar mesons,

$$g_{\sigma B}(\sigma) = g_{\sigma B} b_B \left[1 - \frac{a_B}{2} (g_{\sigma N} \sigma) \right], \quad g_{\sigma^* B}(\sigma^*) = g_{\sigma^* B} b'_B \left[1 - \frac{a'_B}{2} (g_{\sigma^* \Lambda} \sigma^*) \right]. \quad (3)$$

If we set $a_B = 0$ and $b_B = 1$, $g_{\sigma B}(\sigma)$ becomes identical to the σ - B coupling constant in QHD. This is also true of the coupling $g_{\sigma^* B}(\sigma^*)$. Thus, the Lagrangian density in the QMC, QMCg, and CQMC models is given by replacing the σ - B and σ^* - B coupling constants in QHD with the field-dependent couplings, $g_{\sigma B}(\sigma)$ and $g_{\sigma^* B}(\sigma^*)$.

4. Numerical Results

As in the case of QHD, the coupling constants are determined so as to reproduce the saturation properties. We determine the couplings of the vector mesons to the baryons in SU(3) flavor symmetry [12]. For the sake of comparison, we present a calculation based on QHD with the nonlinear (NL) potential, $U_{\text{NL}} = \frac{1}{3}g_2\sigma^3 + \frac{1}{4}g_3\sigma^4$. The coupling constants, g_2 and g_3 , are chosen so as to adjust the values of the incompressibility, K_0 , and effective nucleon mass, M_N^* , in the QMC model.

Table II. Properties of symmetric nuclear matter at the saturation density, $\rho_0 = 0.16 \text{ fm}^{-3}$. The nuclear symmetry energy is also fitted so as to reproduce the empirical data, $E_{\text{sym}}(\rho_0) = 32.5 \text{ MeV}$, in all the cases. The physical quantities are explained in detail in the text.

Model	M_N^*/M_N	K_0 (MeV)	J_0 (MeV)	L (MeV)	K_{sym} (MeV)	K_{asy} (MeV)	$K_{\text{sat},2}$ (MeV)
QHD+NL	0.800	285	-571	88.2	-16.4	-546	-369
QMC	0.800	285	-459	88.2	-17.1	-547	-405
QMCg	0.782	294	-407	89.0	-13.3	-547	-424
CQMC	0.754	309	-320	90.3	-6.3	-548	-455

The properties of symmetric nuclear matter at ρ_0 is presented in Table II. It is found that the effect of gluon and pion decreases M_N^* , while it enlarges K_0 . We also show the third-order incompressibility, J_0 , the slope and curvature parameters of the nuclear symmetry energy, L and K_{sym} , and the 2nd derivative of the isobaric incompressibility coefficient given by $K_{\text{sat},2} = K_{\text{asy}} - \frac{J_0}{K_0}L$ with $K_{\text{asy}} = K_{\text{sym}} - 6L$. The values of K_0 in this study are a little bit larger than the empirical one, and this point would be considered in the future work.

The nuclear binding energy per nucleon in symmetric nuclear and pure neutron matter is shown in the left panel of Fig. 1. We find that, in both cases, the nucleon structure due to quarks and the hyperfine interaction due to gluon and pion increases the binding energy at densities above 0.3 fm^{-3} . In the right panel of Fig. 1, the baryon potentials in symmetric nuclear matter are presented. Although the gluon and pion interactions between two quarks affect the difference among the potentials for Λ and Ξ , it is a little difficult to reproduce the realistic potential for Σ , as already reported in Ref. [10]. In the present study, we adjust the hyperon potentials so as to fit the following values suggested from the experimental data of hypernuclei: $U_\Lambda(\rho_0) = -28 \text{ MeV}$, $U_\Sigma(\rho_0) = +30 \text{ MeV}$, and $U_\Xi(\rho_0) = -18 \text{ MeV}$ [12].

As for the properties of neutron stars, we show the mass-radius relations in Fig. 2. Compared with the QHD+NL and QMC models, the maximum mass of a neutron star is pushed upwards because of the effect of quarks inside a baryon. Additionally, the hyperfine interaction due to the gluon and pion exchanges between two quark enhances the maximum mass in the QMCg and CQMC model. In particular, the pion-cloud effect is remarkably important to support the massive neutron stars. In

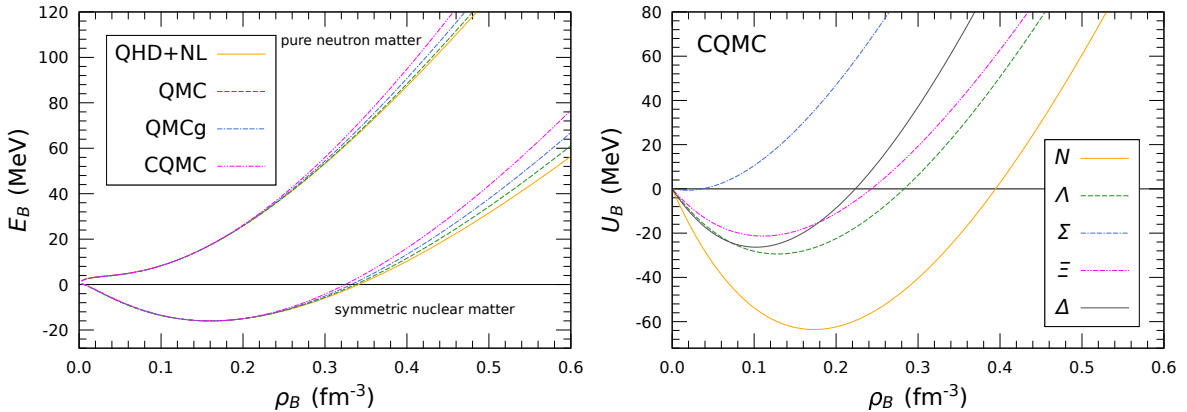


Fig. 1. Nuclear binding energy per nucleon in symmetric nuclear or pure neutron matter (left panel) and potentials for the baryon, $B = N, \Lambda, \Sigma, \Xi, \Delta$, in symmetric nuclear matter (right panel) as a function of the total baryon density, ρ_B .

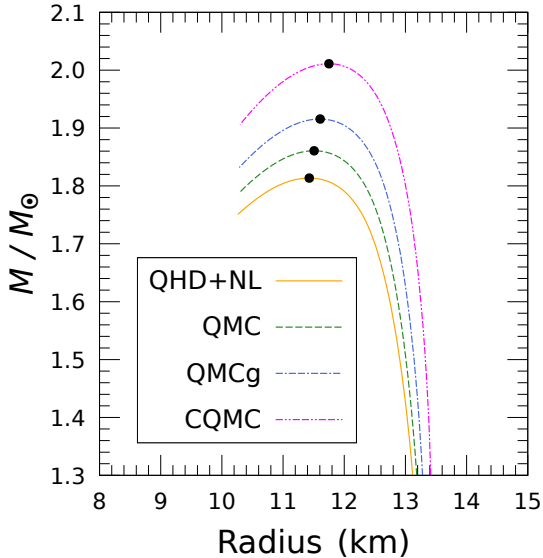


Fig. 2. Mass-radius relations in the QHD+NL, QMC, QMCg, and CQMC models. The filled circle shows the maximum-mass point of a neutron star.

the present calculation, not only nucleons but also hyperons and delta-isobars are taken into account in the core of a neutron star. In all cases, Λ , Ξ^- and Ξ^0 are generated in the core, while the other particles do not appear in the density region below the maximum-mass point.

5. Summary

We have studied the effect of quark degrees of freedom inside a baryon and the hyperfine interaction due to the gluon and pion exchanges between two quarks on the properties of nuclear and neutron-star matter in SU(3) flavor symmetry. It has been found that the variation of baryon substructure in matter plays an important role to support massive neutron stars with hyperons. In particular, the pion-cloud effect is very vital to solve the $2M_{\odot}$ neutron-star problem.

Acknowledgments

This work was supported by JSPS KAKENHI Grant Number JP17K14298.

References

- [1] B. D. Serot and J. D. Walecka, *Adv. Nucl. Phys.* **16**, 1 (1986).
- [2] P. Demorest, T. Pennucci, S. Ransom, M. Roberts, and J. Hessels, *Nature* **467**, 1081 (2010).
- [3] J. Antoniadis *et al.*, *Science* **340**, 6131 (2013).
- [4] B. P. Abbott *et al.* [LIGO Scientific and Virgo Collaborations], *Phys. Rev. Lett.* **119**, 161101 (2017).
- [5] P. A. M. Guichon, *Phys. Lett. B* **200**, 235 (1988).
- [6] K. Saito and A. W. Thomas, *Phys. Lett. B* **327**, 9 (1994).
- [7] K. Saito, K. Tsushima, and A. W. Thomas, *Prog. Part. Nucl. Phys.* **58**, 1 (2007).
- [8] A. W. Thomas, *Adv. Nucl. Phys.* **13**, 1 (1984).
- [9] S. Nagai, T. Miyatsu, K. Saito, and K. Tsushima, *Phys. Lett. B* **666**, 239 (2008).
- [10] T. Miyatsu and K. Saito, *Prog. Theor. Phys.* **122**, 1035 (2010).
- [11] K. Tsushima, K. Saito, J. Haidenbauer, and A. W. Thomas, *Nucl. Phys. A* **630**, 691 (1998).
- [12] T. Miyatsu, M. K. Cheoun, and K. Saito, *Phys. Rev. C* **88**, 015802 (2013).